Quasi-Conservative Lambda Formulation

Andrea Dadone* and Vinicio Magi†
Universitá di Bari, Bari, Italy

The numerical simulation of inviscid transonic flows by means of a "modified lambda formulation" takes into account the shock transition from supersonic to subsonic flow conditions, thus allowing the coupling of the supersonic region with the shocked subsonic one and, as a consequence, the upstream movement of the shock. The present methodology is applied to one- and two-dimensional transonic flows. Although the two-dimensional flow calculations involve Cartesian coordinates and are limited to the thin-airfoil approximation, the method can be generalized to arbitrary two- and three-dimensional flow cases. In all of the computed cases, the shock is found to have appropriate strength and position for steady flow conditions and to move upstream properly when a change in the downstream pressure warrants it.

Introduction

AMONG the several numerical methods developed for the numerical simulation of transonic inviscid flows, the so-called lambda formulation, recently developed and employed by Moretti[1] and Zannetti and Colasurdo,[2] has several very desirable features. The time-dependent, compressible Euler equations are recast in terms of compatibility conditions for characteristic (Riemann) variables along characteristic lines and discretized by means of upwind differences which correctly take into account the direction of wave propagation. In this way a numerical technique is obtained which combines the coding simplicity of finite-difference methods with the intrinsic accuracy and physical soundness of the method of characteristics.

Since its first appearance, the lambda formulation has undergone several improvements. In particular, various implicit integration schemes[3-5] and relaxation methods[6,7] have been developed in order to enhance the efficiency of the lambda methodology by removing the Courant-Friedrichs-Lewy (CFL) stability limitation of the explicit schemes previously employed. Also, a significant improvement in accuracy is achieved by employing a perturbative formulation[8,9] such that only the compressibility effects with respect to a suitable incompressible flow solution need to be computed.

The lambda formulation has its drawbacks; in particular, numerical experiments have shown that for one-dimensional transonic flows the "captured" shock cannot move upstream in the supersonic flow region and that this problem persists in some cases for two-dimensional transonic flows, even if the supersonic bubble is embedded in a subsonic region, which would be expected to allow for upstream propagation. This drawback is due to the decoupling of the supersonic region from the subsonic one once the shock wave is established.

Recently, the "flux-difference splitting,"[10-13] which uses governing equations in conservation form and splits the fluxes according to the wave nature of the flow, has been proposed to solve compressible inviscid flows. A comparison of this methodology with the lambda formulation applied to a system of linear hyperbolic equations[14] shows that they both lead to identical conclusions, but an analysis of the flux-difference splitting applied to the one-dimensional Euler equations demonstrates that it allows a coupling of the supersonic region with the shocked subsonic one by splitting the waves containing a "sonic point," i.e., a vertical characteristic in the (x,t) plane. Such a situation occurs in those mesh intervals where the shock is numerically captured. On the contrary, this basic mechanism is neglected by the classical lambda formulation, but it can be taken into account in order to obtain a modified lambda formulation characterized by a supersonic region coupled with the shocked subsonic one, as done in the present paper.

The method will be first described for one-dimensional flows of a test gas with a specific heat ratio equal to unity; the method will then be extended to classical one-dimensional nonisentropic flows; and finally to the case of nonhomentropic two-dimensional flows within the framework of thin-airfoil theory. The validity and usefulness of the modified lambda methodology will be demonstrated by means of a few example calculations.

Simplified One-Dimensional Flow

Formulation

As regards quasi-one-dimensional inviscid flows of a test gas with a specific heat ratio γ equal to unity, the nondimensional continuity, momentum, and energy equations can be simplified to give

$$Wp_t + W(pu)_x + puW_x = 0 \tag{1}$$

$$W(pu)_t + W(p+pu^2)_x + pu^2 W_x = 0 \tag{2}$$

$$\rho = p \tag{3}$$

where p, ρ, and u are the pressure, density, and velocity of the fluid, respectively; W is the cross-sectional area of the duct; and the subscripts x and t indicate derivatives with respect to the longitudinal coordinate x and time t, respectively. The speed of sound for the flow of the present test gas is constant and set equal to unity.

Equations (1) and (2) can be easily rearranged to give the corresponding lambda formulation equations:

$$C_t + \lambda_c C_x = -\alpha u \tag{4}$$

$$D_t + \lambda_d D_x = \alpha u \tag{5}$$

where α is the specific rate of change of the cross-sectional area W $[\alpha = (dW/dx)/W]$, C and D are the two char-

Presented as Paper 85-0088 at the AIAA 23rd Aerospace Sciences Meeting, Reno, NV, Jan. 14-17, 1985; received Feb. 15, 1985; revision received Nov. 4, 1985.

*Professor, Istituto di Macchine.
†Assistant Professor, Istituto di Macchine.

acteristic Riemann variables, and λ_c and λ_d are the slopes of the corresponding characteristic lines, with

$$C = u + \ell_n p \tag{6}$$

$$D = u - \ell_n p \tag{7}$$

$$\lambda_c = u + 1 \tag{8}$$

$$\lambda_d = u - 1 \tag{9}$$

Let us now consider a transonic nozzle flow. Following the technique suggested in Ref. 13, a flux-difference splitting approach applied to Eqs. (1) and (2) leads to the solution of the Riemann problem sketched in Fig. 1 for the mesh interval *HI* bounded by supersonic flow conditions on the left and by subsonic flow conditions on the right. The Riemann problems to be solved in the two neighboring intervals *GH* and *IL* are also sketched in Fig. 1. The flow in interval *GH* being supersonic, the two waves are both right-running ones and consistently contribute to the evolution in time of mesh point *H*; on the contrary, in interval *IL*, where the flow is subsonic, the two waves have different directions, so that the first one ($1'''$) affects mesh point *I* and the second one ($2'''$) affects mesh point *L*. In interval *HI* the second wave ($2'$) is still right-running and affects mesh point *I*, while the first one ($1'$) simulates a shock and is represented by a converging fan with a vertical characteristic *r*. Such a "converging fan" wave is thus split as follows: the left-running part $r-b$ contributes to the evolution in time of mesh point *H*, whereas the right-running part $a-r$ affects mesh point *I*. In this way the last supersonic mesh point, *H*, is coupled with the shocked subsonic region and the shock can move upstream in the supersonic flow region.

Let us now consider the classical lambda formulation. The corresponding characteristic lines are represented in Fig. 2, where it is shown that characteristics C'' and D'' affect mesh point *H*, characteristics C' and D''' affect mesh point *I*, and finally characteristic C''' affects mesh point *L*. Consequently, the last supersonic mesh point, *H*, is decoupled from the shocked subsonic region and the shock cannot, therefore, move upstream.

Let us now compare Figs. 1 and 2. The wave shapes are different because the converging fan wave $1'$ in Fig. 1 has no corresponding wave in Fig. 2; the classical lambda formulation cannot account for such a wave and its ability to couple the last supersonic mesh point to the subsonic shocked region. From an analytical point of view, by splitting the flux terms, one can rewrite Eqs. (1) and (2) as

$$Wp_t + W(pu)''_x + puW_x + W'(pu)'_x = 0 \tag{10}$$

$$W(pu)_t + W(p+pu^2)''_x + pu^2 W_x + W'(p+pu^2)'_x = 0 \tag{11}$$

where the fourth terms of Eqs. (10) and (11) represent the contribution of the converging fan wave (shock) to the evolution in time of the grid points bounding the mesh interval where it is located; such terms are therefore different from zero only for the interval containing the shock. From a flux-difference splitting point of view, the flux terms corresponding to the converging fan wave are neglected by the lambda formulation. As a consequence, the fourth terms of Eqs. (10) and (11) are considered equal to zero and the corresponding equations are obtained on the basis of the first three terms. However, Eqs. (10) and (11) can be easily rearranged to provide a modified lambda formulation which takes into account this very critical contribution, namely;

$$C_t + \lambda_c C_x = -\alpha u + k_1 \tag{12}$$

$$D_t + \lambda_d D_x = \alpha u + k_2 \tag{13}$$

where

$$k_1 = -\beta[(1-u)f_{1x} + f_{2x}] \tag{14}$$

$$k_2 = \beta[(1+u)f_{1x} - f_{2x}] \tag{15}$$

with

$$f_{1x} = (pu)'_x \tag{16}$$

$$f_{2x} = (p+pu^2)'_x \tag{17}$$

$$\beta = W'/pW \tag{18}$$

In Eqs. (12) and (13), k_1 and k_2 represent corrections with respect to the classical lambda formulation equations, Eqs. (1) and (2), due to the contribution of converging fan waves.

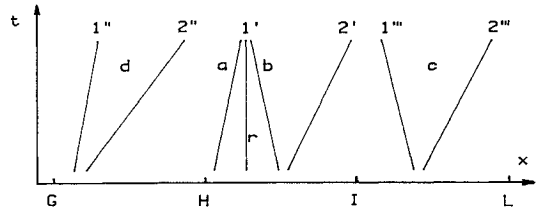

Fig. 1 Riemann problems for $\gamma = 1.0$.

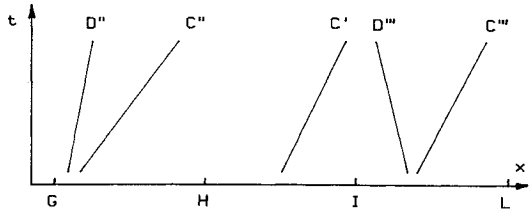

Fig. 2 Characteristic lines for $\gamma = 1.0$.

Numerical Method

Equations (12) and (13) are discretized and linearized in time using the incremental (Δ) approach of Beam and Warming[15] to give

$$\Delta C/\Delta t + \lambda_c^n \Delta C_x + C_x^n \Delta u + \alpha \Delta u = -\lambda_c^n C_x^n - \alpha u^n + k_1^n \tag{19}$$

$$\Delta D/\Delta t + \lambda_d^n \Delta D_x + D_x^n \Delta u - \alpha \Delta u = -\lambda_d^n D_x^n + \alpha u^n + k_2^n \tag{20}$$

In Eqs. (19) and (20) the superscript *n* indicates variables which are evaluated at the old time level t^n explicitly, whereas Δ indicates time increments from the old time level t^n to the new time level $t^{n+1} = t^n + \Delta t$. Moreover, Δu can be eliminated by means of the following relationship:

$$\Delta u = (\Delta C + \Delta D)/2 \tag{21}$$

which can be obtained very easily from Eqs. (3) and (4). The resulting equations are discretized in space by means of a two-point second-order-accurate upwind box scheme[8] as follows. All the terms in Eq. (19), except for k_1, are evaluated at the center of the interval immediately preceding the x_i grid point; that is,

$$\Delta C/\Delta t = (\Delta C_i + \Delta C_{i-1})/2\Delta t \tag{22}$$

$$\lambda_c = (\lambda_{ci} + \lambda_{ci-1})/2 \tag{23}$$

$$C_x = (C_i - C_{i-1})/\Delta x \tag{24}$$

and so on. All the terms in Eq. (20), except for k_2, are evaluated at the center of the interval immediately preceding or following the x_i grid point, in accordance with the supersonic ($u>1$) or subsonic ($u<1$) nature of the flow, respectively.

Let us now consider the correction terms k_1 and k_2. They are different from zero only at the two grid points which bound the interval containing a converging fan wave (i.e., a shock); W' is evaluated at the center of such an interval, while u, p, and W are evaluated at the same point as the other terms of the equation (e.g., at the center of the interval immediately preceding the grid point of the D equation pertaining to the last supersonic grid point, i.e., point H in Fig. 2). The derivatives of the flux terms f given by Eqs. (16) and (17) are evaluated in accordance with the flux-difference splitting methodology.[13] A first-order approximation can be obtained by taking (see Fig. 1)

$$f_x = (f_b - f_r)/\Delta x \tag{25}$$

for the correction terms pertaining to the last supersonic flow grid point, H, and

$$f_x = (f_r - f_a)/\Delta x \tag{26}$$

for the first shocked subsonic grid point, I. According to the D-wave nature of the converging fan wave (1′ in Fig. 1), only fluxes pertaining to D characteristics are considered to obtain a second-order approximation, namely,[13]

$$f_x = (f_b - f_r)/\Delta x - (f_c - f_I)/4\Delta x \tag{27}$$

for the last supersonic flow grid point, H, and

$$f_x = (f_r - f_a)/\Delta x - (f_d - f_G)/4\Delta x \tag{28}$$

for the first shocked subsonic grid point, I. As regards Eqs. (25-28), it is necessary to solve a Riemann problem in the interval containing a converging fan wave to obtain a first-order approximation for the correction terms k_1 and k_2, whereas the Riemann problem solution must be extended to the two neighboring intervals to obtain a second-order approximation. Spurious numerical wiggles, originated near "captured" shocks when a second-order approximation is used, are eliminated by following the criterion suggested by Van Leer.[16]

The following boundary conditions are used. The value of the total pressure is imposed at the inlet of the nozzle (subsonic flow), whereas the static pressure is prescribed at the outlet, if the flow is subsonic.

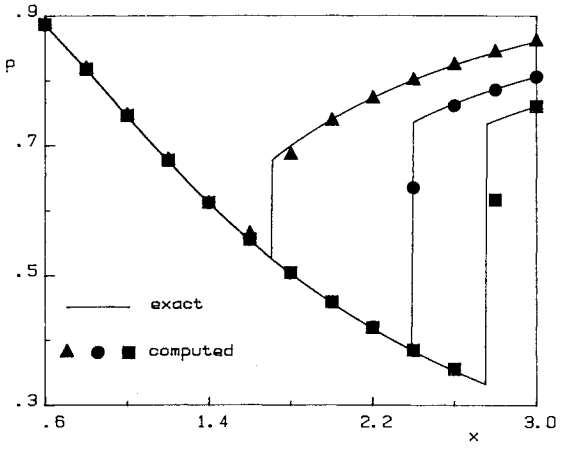

Fig. 3 Nozzle pressure distributions (13 mesh points, $\gamma=1$, $p_{out}=0.76, 0.81, 0.86$).

The discrete internal and boundary equations, obtained as described previously, provide a linear 2×2 block-tridiagonal system for the $2N$ unknowns $C_1,\ldots,C_N$, $D_1,\ldots,D_N$, which is solved very efficiently by standard block-tridiagonal elimination.[17] The solution is then updated and the process is repeated until a satisfactory convergence is reached.

Numerical Results

Three transonic nozzle-flow cases have been considered in order to test the capability of the present methodology to correctly "capture" a shock; a nozzle having a dimensionless cross-sectional area $W=x/2+1/x$ ($0.6\le x\le 3$) with a unitary inlet total pressure and three different values of the outlet static pressure ($p_{out}=0.76$, 0.81, 0.86) has been used to this purpose. Starting from rest, the downstream static pressure is reduced to the prescribed value within a few time steps. The steady-state results obtained by using 13 mesh points are given in Fig. 3, where the pressure numerical results (triangles, circles, and squares) are plotted together with the corresponding exact solutions (lines). The agreement is fair and the shocks are correctly located. To test how the present methodology succeeds in correctly locating the shock as the mesh size is reduced, the three previous test cases have also been computed by using 25, 49, and 97 mesh points; the shocks are still correctly located, as shown, for example, in Fig. 4. where the distributions of pressure and Mach number in the shock region are plotted.

To demonstrate the quasi-conservative nature of the present formulation, the mass flow rate errors (i.e., variations of the mass flow rate across the shock divided by the upstream value) are reported in Table 1.

To test how the present formulation is capable of moving upstream a "captured" shock, the following numerical experiment is performed using 25 mesh points. At first the nozzle outlet pressure is set at the lowest value, 0.76, and a fully converged solution is obtained; the outlet pressure is then raised to the intermediate value and a fully converged solution obtained again; the same procedure is then repeated with the highest value of the outlet pressure and with a value corresponding to subsonic flow conditions inside the nozzle. This numerical experiment shows that the shock moves upstream and positions itself properly in transonic flow conditions, and also correctly disappears in subsonic flow conditions.

The present results have been obtained using the second-order approximation, given by Eqs. (27) and (28), for the derivatives of the flux terms appearing in the correction coefficients k_1 and k_2. Numerical experiments show that a first-order approximation for such derivatives slightly misplaces the position of the shock further upstream in some cases.

Nonisentropic One-Dimensional Flow

Formulation and Numerical Method

For the case of nonisentropic quasi-one-dimensional inviscid flows of a gas with a specific heat ratio not equal to unity, the continuity, momentum, and energy equations can be rearranged to provide the classical nonisentropic lambda formulation equations[18]; with the addition of the correction terms, the following modified dimensionless equations can

Table 1 Mass flow rate errors ($\gamma=1$)

Number of mesh points	Mass flow rate error, %		
	$p_{out}=0.76$	$p_{out}=0.81$	$p_{out}=0.86$
13	2.2	1.9	1.3
25	0.6	1.3	0.5
49	0.6	0.1	0.4
97	0.6	0.2	0.1

be obtained:

$$(C_t - \omega S_t) + \lambda_c (C_x - \omega S_x^c) + \alpha u a = k_1 \tag{29}$$

$$(D_t + \omega S_t) + \lambda_d (D_x + \omega S_x^d) - \alpha u a = k_2 \tag{30}$$

$$S_t + u S_x^u = k_3 \tag{31}$$

where

$$C = u + 2a/(\gamma - 1) \tag{32}$$

$$D = u - 2a/(\gamma - 1) \tag{33}$$

$$\lambda_c = u + a \tag{34}$$

$$\lambda_d = u - a \tag{35}$$

$$\omega = a/\gamma(\gamma - 1) \tag{36}$$

In Eqs. (29-31) S is the entropy; S_x^c, S_x^d, and S_x^u are special space derivatives of the entropy (their finite-difference representation has to be windward with respect to the direction of propagation of the corresponding characteristic line); and k_1, k_2, and k_3 are the correction terms introduced in the present formulation to account for the contribution of converging fan waves. Following a procedure quite similar to the one outlined in the previous section, one can easily obtain such correction terms as

$$k_1 = [1 - (\gamma - 1)u/2a]\, u\beta f_{1x} - [1 - (\gamma - 1)u/a]\, \beta f_{2x} - (\gamma - 1)\beta f_{3x}/a \tag{37}$$

$$k_2 = [1 + (\gamma - 1)u/2a]\, u\beta f_{1x} - [1 + (\gamma - 1)u/a]\, \beta f_{2x} + (\gamma - 1)\beta f_{3x}/a \tag{38}$$

$$k_3 = \gamma[1 - (\gamma - 1)u^2/2a^2]\, \beta f_{1x} + \gamma(\gamma - 1)u\beta f_{2x}/a^2 - \gamma(\gamma - 1)\beta f_{3x}/a^2 \tag{39}$$

where

$$f_{1x} = (\rho u)'_x \tag{40}$$

$$f_{2x} = (p + \rho u^2)'_x \tag{41}$$

$$f_{3x} = \{u[p\gamma/(\gamma - 1) + \rho u^2/2]\}'_x \tag{42}$$

$$\beta = W'/\rho W \tag{43}$$

The same numerical method previously used for Eqs. (12) and (13) is then applied to Eqs. (29-31).

The correction terms k_1, k_2, and k_3 given by Eqs. (37-39) are treated as the correction coefficients k_1 and k_2 in the previous section. In particular, the derivatives of the flux terms f given by Eqs. (40-42) are evaluated by means of Eqs. (25) and (26) or (27) and (28) to obtain a first- or second-order approximation, respectively. In the present flow conditions, however, the subscripts *a, b, c, d, r, G*, and *I* in Eqs. (25-28) refer to Fig. 5, which represents the Riemann problems to be solved for the interval *HI* bounded by supersonic flow conditions on the left and subsonic flow conditions on the right and for the two neighboring intervals *GH* and *IL*. In Fig. 5 the waves 3′, 3″, and 3‴ represent contact surfaces.

The boundary conditions are finally prescribed as follows: at the inlet of the nozzle (subsonic flow) the total temperature and the entropy are assumed to be known, whereas at the outlet the static pressure is imposed if the flow is subsonic.

The discrete internal and boundary equations provide a linear 3×3 block-tridiagonal system which is solved very efficiently by standard block-tridiagonal elimination.[17] An alternate solution method can be devised corresponding to a slightly different time discretization procedure. At first the Riemann variables C and D are evaluated by solving a 2×2 block-tridiagonal system and finally the entropy is determined. Such a procedure has proved to be very efficient as well, and therefore the same idea has been applied to two-dimensional flow calculations.

Numerical Results

The present nonisentropic one-dimensional flow methodology has been applied to the computation of transonic flows of a gas with a specific heat ratio equal to 1.4 inside the same nozzle employed in the previous section. The steady-state results, obtained using 13 mesh points and three different values of the outlet static pressure ($p_{out} = 0.72$, 0.77, 0.82), are given in Figs. 6-8, where the numerical results for

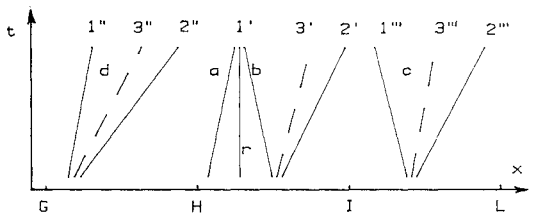

Fig. 5 Riemann problems for $\gamma = 1.4$.

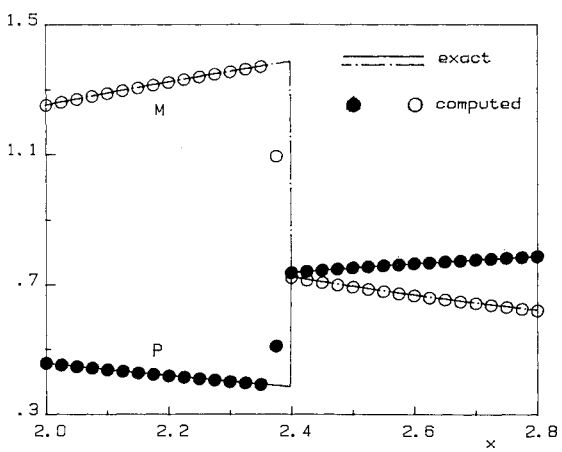

Fig. 4 Nozzle pressure and Mach number distributions in the shock region (97 mesh points, $\gamma = 1$, $p_{out} = 0.81$).

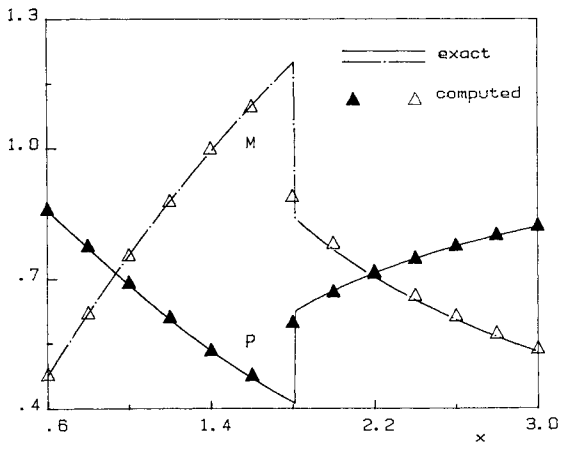

Fig. 6 Nozzle pressure and Mach number distributions (13 mesh points, $\gamma = 1.4$, $p_{out} = 0.82$).

the pressure and the Mach number (triangles, circles, and squares) are plotted together with the corresponding exact solutions (lines). The three previous test cases have also been computed using 25, 49, and 97 mesh points and the computations show that the shocks are still correctly located. The results obtained using 97 mesh points and corresponding to $p_{out} = 0.77$ are plotted in Fig. 9, whereas the total temperature errors (variation of the total temperature across the shock devided by the upstream value) are reported in Table 2.

To test how the present formulation is capable of moving upstream a "captured" shock in the present flow conditions, the numerical experiment outlined in the previous section is repeated. The shock moves upstream and positions itself properly in transonic flow conditions, and it correctly disappears in subsonic flow conditions.

As far as the convergence rate of the method is concerned, an example is given in Fig. 10, where the Mach numbers of the last supersonic flow mesh point and of the following subsonic flow mesh point are plotted vs the number of iterations, K. Satisfactory convergence is obtained in about 10 iterations.

Nonhomentropic Two-Dimensional Flows

Formulation and Numerical Method

The present formulation is limited to the framework of thin-airfoil theory. The first component of the velocity of the fluid can be supersonic, whereas the second one is subsonic everywhere in the flowfield. In such conditions the flux-difference splitting method suggested in Ref. 14 outlines that only one of the four Riemann problems to be solved for evaluating the flux differences can present a wave (simulating a shock) represented by a converging fan with a vertical characteristic. It is a Riemann problem along the first coordinate and presents discontinuities of the entropy, of the speed of sound, and of the first component of the velocity (Fig. 5). This converging fan wave (1′ in Fig. 5) is neglected by the classical lambda formulation for two-dimensional problems too.

Separating the flux terms due to this wave, the dimensionless Euler equations can be written in Cartesian coordinates as

$$\rho_t + (\rho u)''_x + (\rho v)_y + f_{1x} = 0 \tag{44}$$

$$(\rho u)_t + (p + \rho u^2)''_x + (\rho uv)_y + f_{2x} = 0 \tag{45}$$

$$(\rho v)_t + (\rho uv)''_x + (p + \rho v^2)_y + f_{3x} = 0 \tag{46}$$

$$e_t + \{u(p+e)\}''_x + \{v(p+e)\}_y + f_{4x} = 0 \tag{47}$$

In Eqs. (44-47) x, y, and t are the longitudinal and vertical coordinates and time, respectively, and u and v are the longitudinal and vertical velocity components, respectively. Moreover, f_{1x} and f_{2x} are given by Eqs. (40) and (41), whereas f_{3x}, f_{4x}, and e are given by

$$f_{3x} = v(\rho u)'_x = v f_{1x} \tag{48}$$

$$f_{4x} = [u(p+e)]'_x \tag{49}$$

$$e = p/(\gamma - 1) + \rho(u^2 + v^2)/2 \tag{50}$$

Following the procedure outlined in Ref. 2 for the homentropic flow case, one can rearrange Eqs. (44-47) to obtain the modified lambda formulation equations

$$C_t + D_t + (u+a)C_x + vC_y + (u-a)D_x + vD_y = \omega a(S^c_x + S^d_x) + k_1 \tag{51}$$

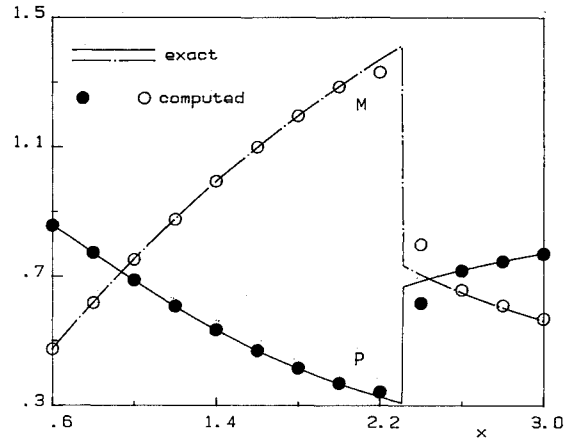

Fig. 7 Nozzle pressure and Mach number distributions (13 mesh points, $\gamma = 1.4$, $p_{out} = 0.77$).

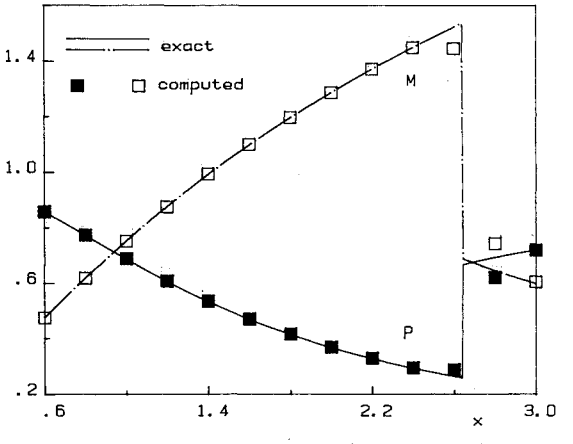

Fig. 8 Nozzle pressure and Mach number distributions (13 mesh points, $\gamma = 1.4$, $p_{out} = 0.72$).

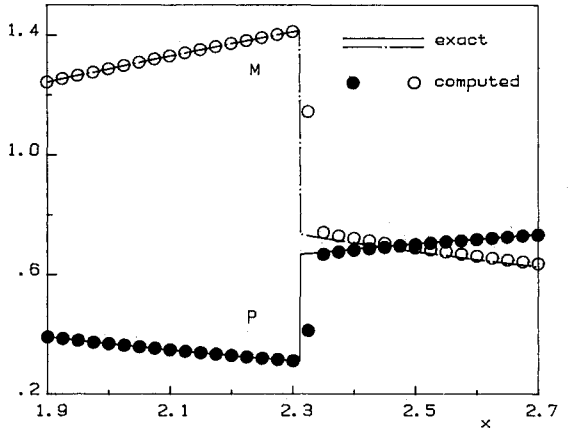

Fig. 9 Nozzle pressure and Mach number distributions in the shock region (97 mesh points, $\gamma = 1.4$, $p_{out} = 0.77$).

Table 2 Total temperature errors ($\gamma = 1.4$)

Number of mesh points	Total temperature error, %		
	$p_{out} = 0.72$	$p_{out} = 0.77$	$p_{out} = 0.82$
13	1.11	0.73	0.09
25	1.57	0.98	0.14
49	0.01	0.90	0.01
97	0.02	0.03	0.14

$$E_t+F_t+uE_x+(v+a)E_y+uF_x+(v-a)F_y$$
$$=\omega a(S_y^e+S_y^f)+k_2 \tag{52}$$

$$C_t-D_t+E_t-F_t+2(u+a)C_x-2(u-a)D_x+2(v+a)E_y$$
$$-2(v-a)F_y=k_3 \tag{53}$$

$$S_t+uS_x^u+vS_y^v=k_4 \tag{54}$$

$$C-D-E+F=0 \tag{55}$$

In Eqs. (51-55) ω is given by Eq. (36) and C, D, E, and F are the four bicharacteristic dependent variables,

$$C=u+2a/(\gamma-1) \tag{56}$$

$$D=u-2a/(\gamma-1) \tag{57}$$

$$E=v+2a/(\gamma-1) \tag{58}$$

$$F=v-2a/(\gamma-1) \tag{59}$$

Moreover, in Eqs. (51-55) S_x^c, S_x^d, S_y^e, and S_y^f are special space derivatives of the entropy, whose finite-difference approximation has to be of the upwind type, based on the direction of propagation of the corresponding bicharacteristic line; S_x^u and S_y^v have the same meaning with reference to the two velocity components of the fluid; and finally k_1, k_2, k_3, and k_4 are the correction terms introduced in the present formulation,

$$k_1=2(uf_{1x}-f_{2x})/\rho \tag{60}$$

$$k_2=0 \tag{61}$$

$$k_3=2[\gamma(v^2-u^2)/a+2a/(\gamma-1)]f_{1x}/\rho$$
$$+4\gamma(uf_{2x}-f_{4x})/\rho a \tag{62}$$

$$k_4=\gamma[1+(\gamma-1)(v^2-u^2)/2a^2]f_{1x}/\rho$$
$$+\gamma(\gamma-1)(uf_{2x}-f_{4x})/\rho a^2 \tag{63}$$

The numerical method described in Ref. 3 is used to linearize the left-hand side of Eqs. (51-54), whereas the right-hand side terms are evaluated at the old time level (explicitly); that is, the left-hand side terms of the governing Eqs. (51-54) are linearized in time and written in incremental form, and the Douglas-Gunn ADI procedure[19] is then applied to the linearized incremental equations. Moreover, Eq. (55) is used to eliminate F in favor of C, D, and E at all stages of the numerical procedure. As in Ref. 3, all the derivatives at the old time level are second-order-accurate three-point windward differences, except at the grid points immediately adjacent to the boundaries, where the derivatives in the direction normal to the boundary are taken as standard central differences. All the derivatives of the incremental variables are instead two-point first-order-accurate windward differences in order to solve only block-tridiagonal systems.

The correction coefficients k_1, k_2, k_3, and k_4 are treated as in the one-dimensional flow case; in particular, the derivatives of the flux terms f given by Eqs. (40), (41), and (49) are evaluated by means of Eqs. (25) and (26) or (27) and (28) to obtain a first- or second-order approximation, respectively. (The subscripts a, b, c, d, r, G, and I appearing in these equations refer to Fig. 5.)

The boundary conditions outlined in Ref. 3 are used with only minor changes. The tangency condition is imposed at the symmetry streamline, at the solid boundary, and at the far-field boundary (for airfoil flow computations). The flow at the inlet boundary being subsonic, three inlet boundary conditions must be prescribed, namely, the entropy, the total temperature, and the transversal velocity component, which is assumed to be zero. The flow at the outlet boundary being subsonic too, only one outlet boundary condition is required; the pressure disturbances produced by the (thin) airfoil or bump are assumed to decay according to small-perturbation theory.

The discrete internal and boundary equations pertaining to the bicharacteristic variables provide, at both sweeps of the ADI procedure, 3×3 block-tridiagonal systems which are solved by standard block-tridiagonal elimination[17] to provide C, D, E, and F. The entropy is then evaluated by solving scalar bidiagonal or tridiagonal systems when sweeping in the x or y direction, respectively.

Numerical Results

The present two-dimensional technique has been applied to the computation of two transonic flow cases. The flow past a symmetric circular-arc airfoil of maximum thickness equal to 10% of the chord with a freestream Mach number equal to 0.83 is considered first. Figure 11 provides the steady-state pressure coefficient results at the airfoil surface: the open and solid circles represent the numerical results obtained with first- and second-order approximations for the correction coefficients, respectively, while the squares in-

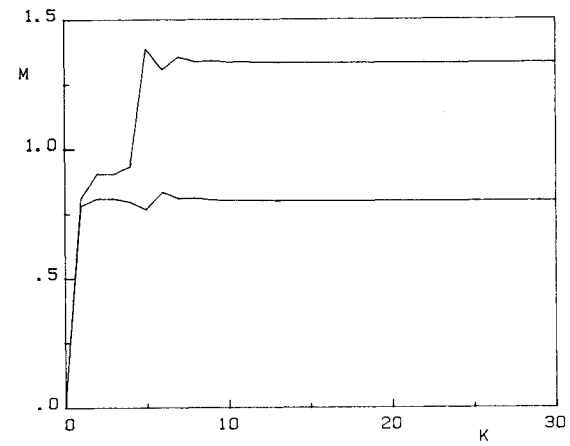

Fig. 10 Nozzle-flow results convergence (13 mesh points, $\gamma=1.4$, $p_{out}=0.77$).

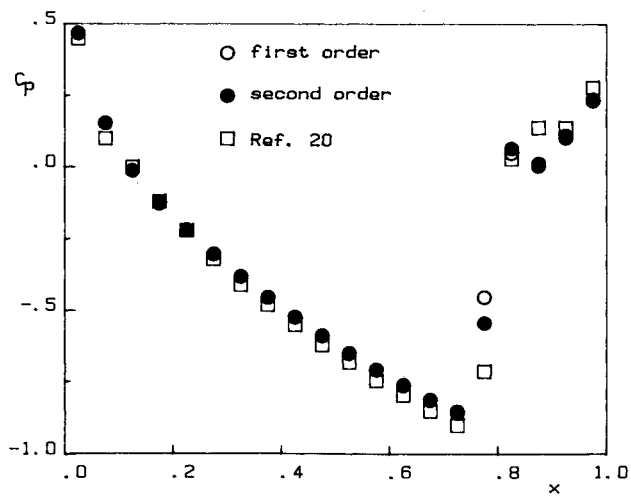

Fig. 11 Pressure coefficient distribution at the airfoil surface.

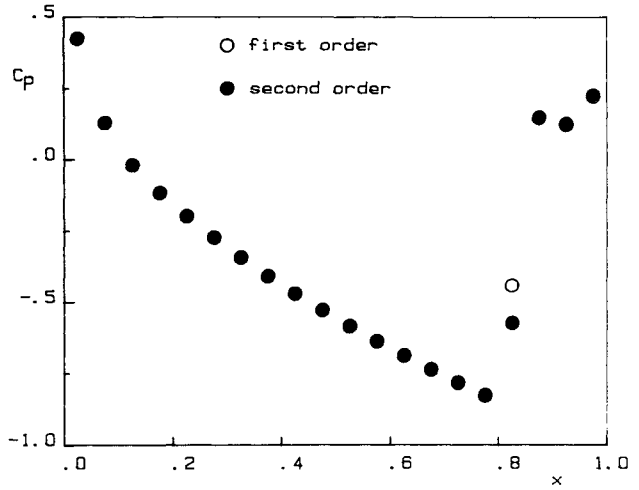

Fig. 12 Pressure coefficient distribution at the bump surface.

dicate the results of Warming and Beam.[20] The agreement is satisfactory and verifies the correctness of the present approach. The present results were obtained using 31×12 grid points in the longitudinal and vertical directions, respectively. The computational grid was stretched ahead of and behind the airfoil and also in the transversal direction, while it is uniform along the surface of the airfoil. The boundary conditions were imposed at distances of 0.64, 1.6, and 4.27 chord lengths ahead of, behind, and above the airfoil, respectively.

The second test case considered in this study is the flow inside a plane channel with a circular bump[21] and characterized by a downstream isentropic Mach number equal to 0.85. The channel geometry is such that the height-to-chord ratio of the circular arc is equal to 0.042 and the ratio of the channel width to such a chord is equal to 2.073. Figure 12 provides the steady-state pressure coefficient results at the bump surface: the open and solid circles represent the numerical results obtained with first- and second-order approximations for the correction terms, respectively. They were obtained using 32×11 grid points in the two directions and a computational grid stretched in the same way as the one employed for the airfoil flow computation, and they are in good agreement with the results of Ref. 21. The boundary conditions were imposed at distances of 0.64 and 2.6 chord lengths ahead of and behind the circular bump, respectively.

Figures 11 and 12 show that the results obtained by using the second-order approximation for the derivatives of the flux terms appearing in the correction coefficients k_1, k_2, k_3, and k_4 differ from those obtained by using the first-order approximation for such derivatives only at the shock. As far as the efficiency of the present methodolgy is concerned, a satisfactory convergence has always been obtained in less than 200 iterations (time cycles) for both test cases considered.

To test how the present formulation is apt to move upstream a "captured" shock in two-dimensional flow conditions, the following numerical experiment is performed. The undisturbed airfoil flow Mach number is set at 0.84 and a converged solution is obtained. The Mach number is then lowered to the correct value equal to 0.83 by changing the asymptotic downstream static pressure, and a converged solution is obtained again. A similar numerical experiment is performed for the bump channel flow too, starting with a downstream isentropic Mach number equal to 0.86. The numerical experiments show that the shock moves upstream and positions itself properly, in perfect agreement with the previously computed results.

Conclusions

A modified lambda formulation capable of correctly computing transonic flows has been provided which allows coupling of the supersonic region with the shocked subsonic region and, as a consequence, the upstream movement of shocks. The major and perhaps unique drawback of the classical lambda methodology has thus been finally eliminated. The proposed formulation was obtained by inserting correction terms into the classical lambda formulation which take into account the transition from supersonic to subsonic flow conditions through a shock.

The proposed methodology was applied to one-dimensional transonic nozzle flows and demonstrated its validity in comparison with exact solutions: The shock is correctly located in steady-state conditions and can move upstream to reach a new, correct steady-state location when the downstream static pressure is changed. The extendability of the present formulation to multidimensional flows was then proved by providing a two-dimensional flow formulation within the framework of thin-airfoil theory, whose validity was demonstrated by means of two test cases; the computed steady-state shock positions are indeed in accordance with published data, and the shock itself can move upstream when the downstream boundary conditions are changed. Current effort is devoted to the extension of the present approach to arbitrary two-dimensional flows,[22] as well as to three-dimensional flows, in order to better assess the capabilities of the present formulation to compute flows of greater engineering interest.

Acknowledgments

This research was supported by the Ministero della Pubblica Istruzione and the Consiglio Nazionale delle Ricerche.

References

[1]Moretti, G., "The λ-Scheme," *Computers and Fluids*, Vol. 7, Sept. 1979, pp. 191-205.

[2]Zannetti, L. and Colasurdo, G., "Unsteady Compressible Flow: A Computational Method Consistent with the Physical Phenomena," *AIAA Journal*, Vol. 19, July 1981, pp. 851-856.

[3]Dadone, A. and Napolitano, M., "An Implicit Lambda Scheme," *AIAA Journal*, Vol. 21, Oct. 1983, pp. 1391-1399.

[4]Dadone, A. and Napolitano, M., "Efficient Transonic Flow Solutions to the Euler Equations," AIAA Paper 83-0258, Jan. 1983; see also "An Efficient ADI Lambda Formulation," *Computers and Fluids*, Vol. 13, No. 4, 1985, pp. 383-395.

[5]Napolitano, M. and Dadone, A., "Three-Dimensional Implicit Lambda Methods," *AIAA Journal*, Vol. 23, Sept. 1985, pp. 1343-1347.

[6]Moretti, G., "Fast Euler Solver for Steady One-Dimensional Flows," *Computers and Fluids*, Vol. 13, 1985, pp. 61-81.

[7]Moretti, G., "A Fast Euler Solver for Steady Flows," AIAA Paper 83-1940, July 1983.

[8]Dadone, A. and Napolitano, M., "Accurate and Efficient Solutions of Compressible Internal Flows," AIAA Paper 84-1247, June 1984; see also, *Journal of Propulsion and Power*, to be published.

[9]Dadone, A. and Napolitano, M., "A Perturbative Lambda Formulation," *Lecture Notes in Physics*, Springer-Verlag, Berlin, Vol. 218, 1985, pp. 175-179.

[10]Roe, P. L., "The Use of the Riemann Problem in Finite Difference Schemes," *Lecture Notes in Physics*, Springer-Verlag, Berlin, Vol. 141, 1981, pp. 354-359.

[11]Osher, S. and Solomon, F., "Upwind Difference Schemes for Hyperbolic Systems of Conservation Laws," *Mathematics of Computation*, Vol. 38, 1982, pp. 339-377.

[12]Lombard, G. K., Oliger, J., and Yang, J. Y., "A Natural Conservative Flux Difference Splitting for the Hyperbolic Systems of Gasdynamics," AIAA Paper 82-0976, June 1982.

[13]Pandolfi, M., "A Contribution to the Numerical Prediction of Unsteady Flows," AIAA Paper 83-0121, Jan. 1983.

[14]Pandolfi, M., "On the Flux-Difference Splitting Method in Mutidimensional Unsteady Flows," AIAA Paper 84-0166, Jan. 1984.

[15]Beam, R. M. and Warming, R. F., "An Implicit Factored Scheme for the Compressible Navier-Stokes Equations," *AIAA Journal*, Vol. 16, April 1978, pp. 393-402.

[16]Van Leer, B., "Towards the Ultimate Conservative Difference Scheme. IV. A New Approach to Numerical Convection," *Journal of Computational Physics*, Vol. 123, March 1977, pp. 276-299.

[17]Isacson, E. and Keller, H. B., *Analysis of Numerical Methods*, Wiley, New York, 1966.

[18]Zannetti, L., "Numerical Treatment of Boundaries in Compressible Flow Problems," Fourth GAMM Conference, Paris, Oct. 1981.

[19]Douglas, J. and Gunn, J. E., "A General Formulation of Alternating Direction Methods," *Numerische Matematik*, Vol. 6, 1964, pp. 428-453.

[20]Warming, R. F. and Beam, R. M., "Upwind Second-Order Differences Schemes for Applications in Aerodynamic Flows," *AIAA Journal*, Vol. 14, Sept. 1976, pp. 1241-1249.

[21]Rizzi, A. and Viviand, H. (eds.), "Numerical Methods for the Computation of Inviscid Transonic Flows with Shock Waves," *Notes on Numerical Fluid Mechancis*, Vol. 3, 1981.

[22]Dadone, A., "Accurate and Efficient Solutions of Transonic Internal Flows," AIAA Paper 85-1334, July 1985.